








Zero voltage switching with reduced current stress for LED lighting applications

Kambhampati Venkata Govardhan Rao^{1,2}  | Malligunta Kiran Kumar²  |
 B. Srikanth Goud³  | Ramanjaneya Reddy Udumula⁴  | Ch. Rami Reddy^{5,6}  |
 Praveen Kumar Balachandran^{7,8}  | Muhammad Ammirul Atiqi Mohd Zainuri⁷  |
 Suganthi Ramasamy⁹

¹Department of Electrical and Electronics Engineering, St. Martin's Engineering College, Secunderabad, Telangana, India

²Department of Electrical and Electronics Engineering, Koneru Lakshmaiah Education Foundation, Vijayawada, Andhra Pradesh, India

³Department of Electrical and Electronics Engineering, Anurag University, Hyderabad, Telangana, India

⁴Department of Electrical and Electronics Engineering, SRM University-AP, Mangalagiri, Andhra Pradesh, India

⁵Department of Electrical and Electronics Engineering, Joginapally B. R. Engineering College, JNT University, Hyderabad, India

⁶Applied Science Research Center, Applied Science Private University, Amman, Jordan

⁷Department of Electrical, Electronics and Systems Engineering, Faculty of Engineering and Built Environment, Universiti Kebangsaan Malaysia, Selangor, Malaysia

⁸Department of Electrical and Electronics Engineering, Chennai Institute of Technology, Chennai, Tamilnadu, India

⁹Department of Electrical and Electronic Engineering (DIEE), University of Cagliari, Cagliari, Italy

Correspondence

Suganthi Ramasamy, Department of Electrical and Electronic Engineering (DIEE), University of Cagliari, Cagliari, Italy.
 Email: suganthi.ramasamy@unica.it

Abstract

Lighting systems using light emitting diode (LED) have drawn significant attention across the world. Nevertheless, to maintain a steady light output, these systems necessitate constant current regulators. This article proposes a buck–boost integrated zero voltage switched full-bridge LED converter with low current stress. It powers two identical lamps and a lamp of power rating twice the identical lamp. A direct current voltage source, arranged in series, transmits a portion of light power without conversion. A regulated low power output is provided using a complete bridge converter. The semiconductor switches off the full-bridge converter carry minimal current. This characteristic lowers conduction losses. The suggested converter facilitates dimming operation via on–off control and zero voltage switching, leading to minimal switching losses. Further input voltage of full-bridge converter is modulated to maintain constant LED lamp current. The detailed steady-state analysis and implementation of the proposed full-bridge LED converter with dimming control operation is presented here.

1 | INTRODUCTION

Light emitting diodes (LEDs) are quickly displacing traditional light sources in many different kinds of lighting, including home, street, car, and ornamental applications, due to their improved lifespan, compactness, light efficiency per watt, envi-

ronmental friendliness, and colour rendering [1]. LEDs are quickly occupying traditional light sources in domestic lighting, municipal lighting, automotive, ornamental, and industry lighting due to their benefits. Many LED applications require steady and regulated operating current [2, 3]. Mostly switched mode power electronic converters are preferred to power LED

This is an open access article under the terms of the [Creative Commons Attribution](https://creativecommons.org/licenses/by/4.0/) License, which permits use, distribution and reproduction in any medium, provided the original work is properly cited.

© 2024 The Author(s). *IET Power Electronics* published by John Wiley & Sons Ltd on behalf of The Institution of Engineering and Technology.

lighting systems [4]. DC-fed LED driver topologies have been reported in the recent past [5–10]. The proliferation of electronic devices in residential, commercial, and occupational settings is driving the increasing use of DC power distribution [5, 6]. The power converter structure is simplified. Thus, DC-fed LED drivers are more appealing and a research area [7, 8]. Additional DC-fed LED drivers with soft-switching reduce lighting system space [9]. Different soft-switched DC-fed LED converter systems are proposed for lighting [10]. In addition, to handle the AC–DC power imbalance, electrolytic capacitors (EC) are necessary [11]. The total size of the driver increases, and efficiency drops as the number of components increases due to more power conversion steps. Reduced power converter stages and elimination of EC are results of DC grid power distribution [12]. The system's efficiency and dependability are enhanced as a result. In lighting systems, these benefits are particularly appealing for the application of high-brightness LEDs (HB-LEDs). As a result, DC-grid-fed LED topologies have emerged as a hot area for academic enquiry [13].

From the literature, two voltage levels will be used by futuristic advanced DC grid for commercial, residential, institutional uses, and applications requiring little power, such as mobile phone charging, personal computers, bedside lights, and battery chargers, use 48 V supplies; applications requiring high power, such as washing machines, heaters, ACs, main lighting, and so on, utilize 380 V supplies, which range from 360 to 400 V [14]. Numerous studies have proposed AC-grid-powered LED drivers with power factor correction (PFC). A substantial electrolytic capacitor (EC) is required to balance the direct current output power with the instantaneous input power, together with a high step-down converter to generate a low direct current voltage from the alternating current grid supply [15]. An absence of literature proposes coupled inductor methods for high step-down conversion gains. On the other hand, because of leakage energy in the linked inductor, the topologies shown in [16, 17] experience large switching spikes across the switch. Reducing switching spikes across the switch, the authors of reference [4] suggested a topology to recycle this leakage energy. Conventionally, single-stage and two-stage power conversion topologies use the AC-grid-supplied LED drivers. Reduced component count, simplified control, and a single power processing step are the benefits of single-stage LED drivers. There is a risk of significant conduction and switching loss due to the large potential and current stresses experienced by the switching devices. In addition, numerous writers have introduced AC-grid-fed LED drivers that use PFC, mitigating issues with EC and enhancing dimming capabilities, among other things. The soft switching converters and comparative studies for overcoming the voltage fluctuations [18–20]. A bidirectional converter (BDC) solar powered LED street light system in [3] and with the non-isolated wide range converter of LED driver [21] are enhanced. Improving the overall driver's lifespan by doing away with EC is the work's main contribution. But more BDC is needed, which means more components and more money. Most of the authors discussed AC-grid-fed LED drivers. Nevertheless, to further the applications of the new DC grid power distribution, only a limited number of

authors have proposed DC-grid-powered LED drivers [7, 22]. The full-bridge converter proposed in reference [23] achieves input regulation using phase shift control. This design can power numerous bulbs, rendering it appropriate for high-power applications. However, the higher number of components per lamp increases the cost, and the presence of a transformer causes bulkier size and increases losses. The isolated a current-fed Capacitor - Inductor - Inductor- Capacitor (CLLC) resonant converter introduced in reference [24] achieves soft switching and reduces the number of magnetic components by utilizing the transformer's magnetizing and leakage inductance as primary resonant components. The LED current is controlled by modifying the duty cycle of the primary switches, enabling functionality across a broad spectrum of input voltages. The LED driver in reference [25] consists of a full-bridge configuration with two synchronous boost converters operated in parallel and a buck–boost converter. The synchronous boost converters in the full bridge are phase shifted by 180 degrees and operate with a fixed duty cycle. The parallel operation of the boost converters helps in reducing source current ripple. Moreover, the smooth switching of devices in boost converters yields enhanced efficiency. However, the integration of paralleled boost converters with a full-bridge feeding a buck–boost converter adds complexity to the circuit design, making it more difficult to implement and troubleshoot. A three-leg asymmetrical voltage resonant converter developed for independent dimming control is presented in reference [26]. The converter can independently power several loads and includes a dimming feature. The principal innovations of the proposed LED driver encompass autonomous dimming control, asymmetrical voltage regulation, zero voltage switching (ZVS) for all power switches, and improved efficiency. The threshold voltage for the LED loads is supplied by batteries arranged in series with the LED loads, hence minimising power processing demands for the proposed converter. An Line-Commutated Converters (LCC)-based resonant converter with an inherent load-independent output current characteristic is described for automotive LED driver applications in reference [27].

This paper contributes an input modulated zero voltage switched full-bridge converter with less device current stress for LED lighting applications. It powers two identical lamps and a lamp of power rating twice the identical lamp. The current stress of devices in full-bridge converter is very less and they are switched at zero voltage. These characteristics enhance the overall efficiency of the proposed full-bridge LED converter. LEDs do not conduct below threshold voltage; this feature is utilized in the proposed converter. Hence the processing power by the converter is reduced. Further, in the proposed configuration, additional inductor or capacitor or their combinations are not used to achieve ZVS.

Further, this paper, organized with the proposed ZVS converter is presented in Section 2, after the introduction in Section 1. In Section 3, the modes of operation for the proposed converter and the design techniques with loss analysis are elaborated in Section 4. Section 5 deals with the dimming control techniques and its regulation feature. Finally, Section 6 presents the numerical simulation results along with experimental results

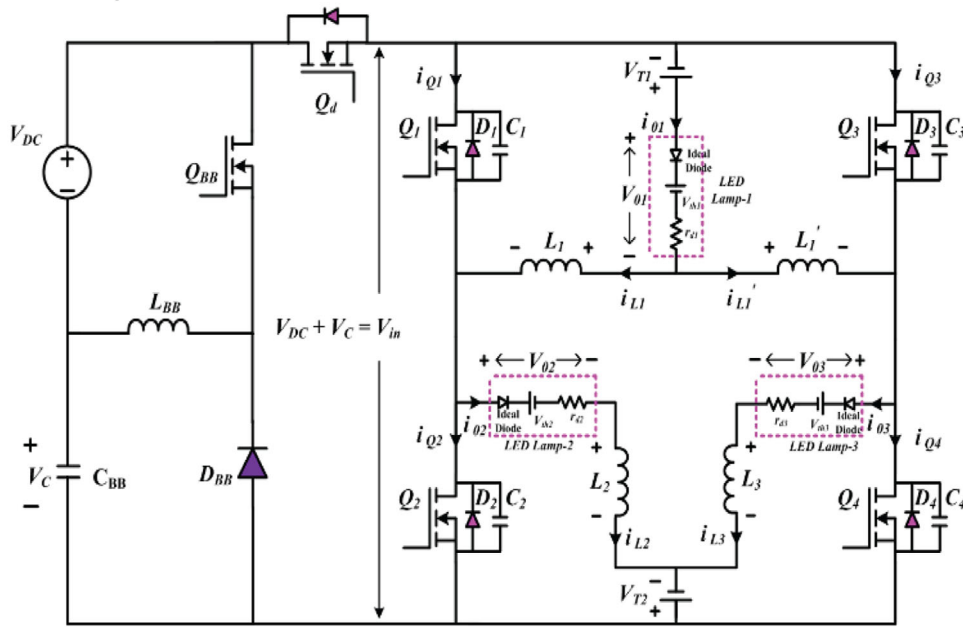


FIGURE 1 The proposed soft-switching converter.

and comparative analysis. Section 7 delivers the conclusion of this proposed technique along with the future scope.

2 | PROPOSED ZERO VOLTAGE SWITCHING CONVERTER

Figure 1 shows the proposal complete bridge LED converter. It has a complete bridge with four power MOSFETs (Q_1 , Q_2 , Q_3 , and Q_4). MOSFETs have intrinsic body diodes and output capacitance. The converter uses three LED bulbs. L_1 and L'_1 interleaving inductors power LED lamp-1. A DC voltage (V_{T1}) below lamp-1's threshold voltage is placed in series. Because of 180° out-of-phase current in inductor L_1 and L'_1 , lamp-1 has ripple-free current. Lamp-1 receives half the power from inductors L_1 and L'_1 . LED lamp-2 and lamp-3 are identical. Series connection of L_2 , lamp-2, and V_{T2} parallels Q_2 . Q_4 is parallel to inductor L_3 , lamp-3, and V_{T2} . V_{T2} must be below lamp-2 or lamp-3's threshold voltage. To mitigate current stress and thrive ZVS in MOSFETs (Q_1 – Q_4), lamp-1's power rating is double that of lamp-2 or lamp-3. Full-bridge devices lose less conduction and switching with this feature. The suggested LED converter regulates LED lamp currents with a buck-boost converter. It modifies V_{in} , the complete bridge circuit's input voltage. LED bulb dimming switch Q_d turns the complete bridge circuit on and off at low frequency.

3 | MODES OF OPERATION FOR PROPOSED CONVERTER

As a future LED driver for DC grid applications, this article suggests a zero voltage switched full-bridge converter. Within the framework of the DC grid, the suggested converter topology is

examined, and a comprehensive steady-state analysis is offered. The dimming function allows it to supply lamps with varying power ratings. The full-bridge converter's semiconductor switches share the current equally between lamp-2 and lamp-3, and the interleaved inductor means that they only conduct a tiny current when turned on. With this function, conduction losses are decreased. The proposed converter exhibits negligible switching losses owing to its ZVS operation. The increased efficiency is a consequence of the decreased switching and conduction losses. Not only that, but this setup allows for dimming via on/off control and uses less components per lamp. The proposed soft-switching converter can be operated in four operating modes, with their operating duration. Figure 2 illustrates the analogous circuit schematics for the individual mode of operation.

3.1 | Mode I

This mode of operation is performed during $t = t_0$, the gate control signals are applied for Q_1 and Q_4 . Inductors L'_1 and L_2 charge linearly and inductors L_1 and L_3 discharge linearly. During t_0 – t_1 , the Q_1 carries a current of $(i_{L2} - i_{L1})$ and the Q_4 carries a current of $(i'_{L1} - i_{L3})$. Consequently, the present stress and conduction losses of Q_1 and Q_4 are markedly reduced. This option activates trimming when Q_1 and Q_4 are off at $t = t_1$. The current i'_{L1} , i_{L1} , i_{L2} , and i_{L3} can be acquired from Equations (1)–(4) as below.

$$i_{L1}(t) = i_{L1}(t_0) + \frac{-V_{01} + V_{T1}}{L_1}(t - t_0) \quad (1)$$

$$i'_{L1}(t) = i'_{L1}(t_0) + \frac{V_{in} + V_{T1} - V_{01}}{L'_1}(t - t_0) \quad (2)$$

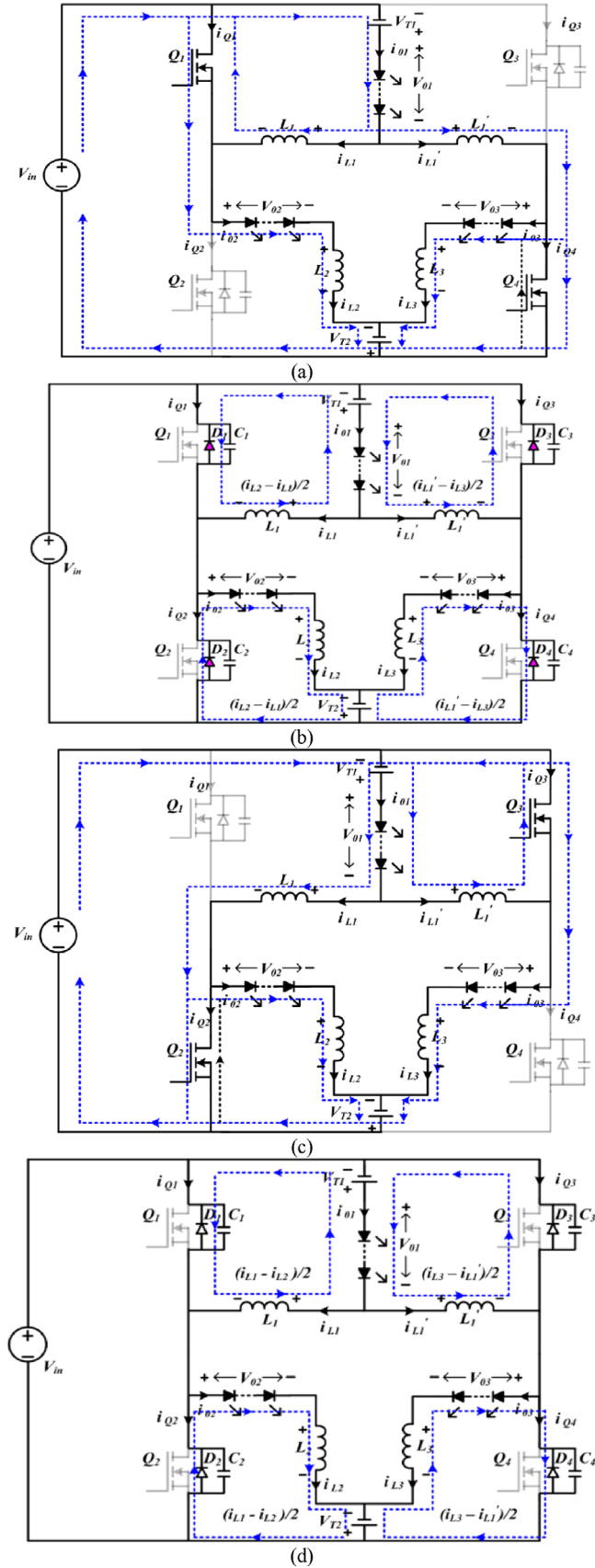


FIGURE 2 Analogous circuits of the proposed converter: (a) Mode I. (b) Mode II. (c) Mode III. (d) Mode IV.

$$i_{L2}(t) = i_{L2}(t_0) + \frac{V_{in} + V_{T2} - V_{02}}{L_2}(t - t_0) \quad (3)$$

$$i_{L3}(t) = i_{L3}(t_0) + \frac{-V_{03} + V_{T2}}{L_3}(t - t_0) \quad (4)$$

3.2 | Mode II

This mode of operation is performed during $t_1 = t_2$, the gate voltages for Q_1 and Q_4 are removed at zero voltage. There is no change to the state of the switches Q_2 and Q_3 . During the interval from t_1 to t_2 , the currents $(i_{L2} - i_{L1})/2$ and $(i_{L1'} - i_{L3})/2$, originating from zero to the input voltage, charge the drain-to-source capacitances C_1 and C_4 , respectively. Simultaneously, the input voltage is diminished to zero by discharging the drain-to-source capacitances C_2 and C_3 using currents $(i_{L2} - i_{L1})/2$ and $(i_{L1'} - i_{L3})/2$, respectively. D_2 and D_3 , which are switch body diodes, are subsequently turned on. For a zero voltage turn-on, the gate voltages of Q_2 and Q_3 can now be provided. This mode activates at $t = t_2$, at the completion of charging and discharging of capacitances, as delineated in Equations (5) and (6).

$$C_1 = C_2 = \frac{(i_{L2} - i_{L1})}{2V_{in}}(t_2 - t_1) = \frac{(i_{L2} - i_{L1})t_{d1}}{2V_{in}} \quad (5)$$

$$C_3 = C_4 = \frac{(i_{L1'} - i_{L3})}{2V_{in}}(t_2 - t_1) = \frac{(i_{L1'} - i_{L3})t_{d1}}{2V_{in}} \quad (6)$$

3.3 | Mode III

This mode of operation is performed during $t_2 = t_3$, gate voltages are applied for Q_2 and Q_3 at $t = t_2$. Inductors L_1' and L_2 discharge linearly and inductors L_1 and L_3 charge linearly. During $t_2 - t_3$, switch Q_2 carries a current of $(i_{L1} - i_{L2})$ and Q_3 carries a current of $(i_{L3} - i_{L1}')$. Consequently, the present stress and conduction losses of Q_2 and Q_3 are markedly reduced. This mode activates trimming when Q_2 and Q_3 are deactivated at $t = t_3$, as shown by Equations (7) and (8).

$$i_{L1}(t) = i_{L1}(t_2) + \frac{V_{in} - V_{01} + V_{T1}}{L_1}(t - t_2) \quad (7)$$

$$i_{L1}'(t) = i_{L1}'(t_2) + \frac{V_{T1} - V_{01}}{L_1'}(t - t_2) \quad (8)$$

3.4 | Mode IV

Between t_3 and t_4 , switches Q_2 and Q_3 are deactivated while switches Q_1 and Q_4 are activated at zero voltage. This technique is analogous to that in mode II. This mode terminates at $t = t_4$ at the completion of charging and discharging of capacitances, as seen in Equations (9) and (10).

$$C_1 = C_2 = \frac{(i_{L1} - i_{L2})}{2V_{in}}(t_4 - t_3) = \frac{(i_{L1} - i_{L2})t_{d2}}{2V_{in}} \quad (9)$$

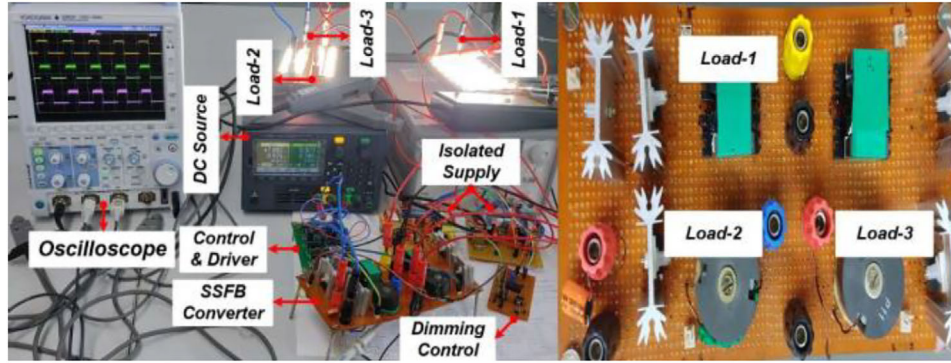


FIGURE 3 Experimental setup.

$$C_3 = C_4 = \frac{(i_{L3} - i'_{L1})}{2V_{in}}(t_4 - t_3) = \frac{(i_{L3} - i'_{L1})t_{d2}}{2V_{in}} \quad (10)$$

4 | DESIGN TECHNIQUES AND LOSS ANALYSIS

The suggested full-bridge LED driver is evaluated using the following assumptions:

- The LED driver functions in a steady condition.
- The switches employed are ideal.
- Continuous conduction mode.
- A uniform voltage is applied across all the LED lights.

4.1 | For lamp-1 and its parameters

The proposed full-bridge LED converter powers lamp-1 by interleaving. This section includes lamp-1 rating, interleaved inductor calculations, and input voltage. Lamp-1 specifications must be selected using an LED equivalent circuit. This study uses TMX HP 3W LED's shown in Figure 3. TMX HP 3W LED V-I features are given. The LED cut-in voltage (V_{th}) is 2.3 V, with an operational point established at 3.42 V and 0.59 A. Each of Lamp-1's four strings has seven LEDs in sequence. Thus, each main bulb operates at 23.94 V, 2.36 A, and 56 W. The cut-in voltage of each main bulb is 16.1 V. V_{o1} of lamp-1 is 23.94 V and i_{o1} is 2.36 A. As said, LED lamp-1 has a DC voltage source (V_{T1}) in series that must be smaller than its cut-in voltage because LED lamps are not conducted below it. Therefore, 12 V is chosen. Full-bridge converter supplies 11.94 V. Given a duty ratio (D) of 0.5, V_{T1} of 12 V, and V_{o1} of 23.94 V, the input voltage is determined using Equation (11).

$$V_{in} = \frac{23.94 - 12}{0.5} \cong 24V, \quad (11)$$

Given a V_{in} of 24 V, V_{T1} of 12 V, V_{o1} of 23.94 V, D of 0.5, a switching period T of 5 μ s, and a current ripple of 1.4 A, the

inductance L_1 is computed as Equation (12).

$$L_1 = L'_1 = \frac{(-23.94 + 12)}{(1.4)} \cdot (1 - 0.5) \cdot 5 \cdot 10^{-6} \cong 22 \mu H \quad (12)$$

4.2 | For lamp-2 and lamp-3 and parameters

Lamp-2 and lamp-3 in the suggested complete bridge LED converter are functionally equivalent and draw power from the buck operation. This section details the lamp-2 rating, how to calculate the value of the inductor (L_2), and the input voltage. It is decided that $V_F = 3.42$ V and $I_F = 0.59$ A will be the operating points for lamp-2. It has two strings that run parallel to each other, with seven LEDs linked in series on each string. As a result, the operating parameters for lamp-2 are 23.94 V, 1.18 A, and 28 W. Lamp-2's cut-in voltage comes out to 16.1 V. Hence V_{T2} is selected as 12 V. The output voltage (V_{o2}) of lamp-1 is measured at 23.94 V, while the output current (i_{o2}) through lamp-1 is recorded at 1.18 A. The input voltage V_{in} can also be determined, as expressed in Equation (13).

$$V_{in} = \frac{23.94 - 12}{0.5} \cong 24V \quad (13)$$

Given a V_{in} of 24 V, V_{T2} of 12 V, V_{o2} of 23.94 V, a duty cycle D of 0.5, a switching period T of 5 μ s, and a current ripple of 8.7% of i_{o2} , the inductance L_2 is computed as Equation (14).

$$L_2 = L_3 = \frac{(-23.94 + 12)}{(8.7\%) \times 1.18} \cdot (1 - 0.5) \cdot 5 \cdot 10^{-6} \cong 292 \mu H \quad (14)$$

4.3 | Loss analysis

The loss analysis of the proposed converter is conducted by disregarding inductor core losses. The switching losses in devices inside a full bridge are low due to ZVS turn-on and turn-off. Therefore, only conduction losses are taken into account in full-bridge switching devices.

The cumulative Metal Oxide Semiconductor Field Effect Transistor (MOSFET) conduction losses in the proposed converter are determined using the subsequent equation.

$$P_Q = i_{Q1\text{rms}}^2 r_{ds1} + i_{Q2\text{rms}}^2 r_{ds2} + i_{Q3\text{rms}}^2 r_{ds3} + i_{Q4\text{rms}}^2 r_{ds4} + i_{Q\text{BBrms}}^2 r_{ds\text{BB}} \quad (15)$$

Five inductors are employed in the configuration. The cumulative loss incurred in inductors is determined using the subsequent equation.

$$P_L = i_{L1\text{rms}}^2 r_{L1} + i_{L1'\text{rms}}^2 r_{L1'} + i_{L2\text{rms}}^2 r_{L2} + i_{L3\text{rms}}^2 r_{L3} + i_{L\text{BBrms}}^2 r_{L\text{BB}} \quad (16)$$

The loss in diode in buck–boost converter is expressed as

$$P_D = P_{RF} + P_{VF} \quad (17)$$

Cumulative loss in the converter is given by

$$P_{\text{Loss}} = P_Q + P_L + P_D \quad (18)$$

Cumulative power output is given by

$$P_0 = P_{01} + P_{02} + P_{03} \quad (19)$$

Therefore, the overall efficiency of the suggested LED driver topology is determined as

$$\eta = \frac{P_0}{P_0 + P_{\text{Loss}}} \quad (20)$$

The loss distribution of the suggested LED driver components at a specified power level of 112 W is illustrated in the figure. At $P_0 = 112$ W, the cumulative losses amount to 4.188 W. The power losses for switches Q_1, Q_2, Q_3, Q_4 , and Q_{BB} are 0.12132, 0.12132, 0.12132, 0.12132, and 0.616 W, respectively. The losses for the inductors L_1, L_1', L_2, L_3 , and L_{BB} are recorded as 0.2972, 0.2917, 0.4539, 0.4368, and 0.713 W, respectively. The power loss in the diode switch (D_{BB}) used for dimming control is 0.89 W.

5 | DIMMING CONTROL TECHNIQUES AND ITS REGULATION FEATURES

LED lighting applications save power with dimming control. The two most common LED dimming mechanisms are amplitude modulation (AM) and pulse width modulation (PWM). In amplitude modulation (AM), the direct current is regulated by LED strings, facilitating dimming capabilities. Conversely, PWM dimming controls the average current by alternating the on/off cycling of LEDs at a standard current and low frequency. By linking a switch Q_d in series with input, the proposed LED converter can be made to dim by means of a low-frequency gate signal that activates and deactivates the bridge converter. Since each LED light has the same average current, brightness can be regulated. Dimming is set at 100 Hz to eliminate flickers.

TABLE 1 Parameters of the converter.

DC input voltage, V_{in}	24 V
DC voltage source, V_{T1}, V_{T2}	12 V
Number of LEDs	56
LED operating current, I_{operated}	590 mA
Switching frequency, f_s	200 kHz
Duty ratio of switches in bridge configuration	0.5
L_1, L_1'	22 μH
L_2, L_3	292 μH
PWM dimming frequency	100 Hz
Duty ratio of dimming switch Q_d	0 to 1
Frequency of buck–boost converter	100 kHz
Switching devices used	MOSFET IRF640N
Control ICs used	UC 3875 and SG 3525
Driver ICs used	IR 2110, IR 2117, and MIC4425

The variations in voltages V_{DC}, V_{T1} , and V_{T2} change the LED lamp current magnitude. To maintain lamp current constant, input voltage to bridge circuit V_{in} must be constant. To maintain V_{in} constant, buck–boost converter with modification is connected at the input side. It produces V_C , which is a controllable voltage. This controllable voltage V_C compensates the variations in V_{DC}, V_{T1} , and V_{T2} .

6 | SIMULATION AND EXPERIMENTAL RESULTS

An experimental prototype of 112 W was developed to test the steady-state performance of the proposed buck–boost integrated ZVS full-bridge DC–DC converter, utilising the parameters and specifications given in Table 1. Figure 3 illustrates an experimental model of the proposed project. The block diagram of the control circuit for the suggested arrangement is illustrated in Figure 4. The PWM controller IC UC3875 generates gate voltages for the whole bridge. The gate voltage for the switch (Q_{BB}) and the dimming switch (Q_d) is produced by a PWM controller integrated circuit, SG 3525. The sum of V_{DC} and V_C equals 24 V, which serves as the input voltage (V_{in}) for the proposed full-bridge converter. LED lamp-1 is designed to operate at 56 W, while LED lamp-2 and LED lamp-3 are intended to function at 28 W each.

Figures 5 and 6 depict the modelling and experimental waveforms of gate voltages ($V_{gs1} - V_{gs4}$), lamp currents (i_{o1}, i_{o2} , and i_{o3}), and lamp voltages (V_{o1}, V_{o2} , and V_{o3}) under full illumination. Figures 5 and 6 clearly demonstrate that the modelling and experimental results are in close concordance. Additionally, it is seen that lamp-1 exhibits no voltage or current ripple, but LED lamp-2 and lamp-3 have little ripple.

Figures 7 and 8 illustrate the simulation and experimental waveforms of the switch voltages and switch currents for the proposed LED driver. Figures 7 and 8 demonstrate that the

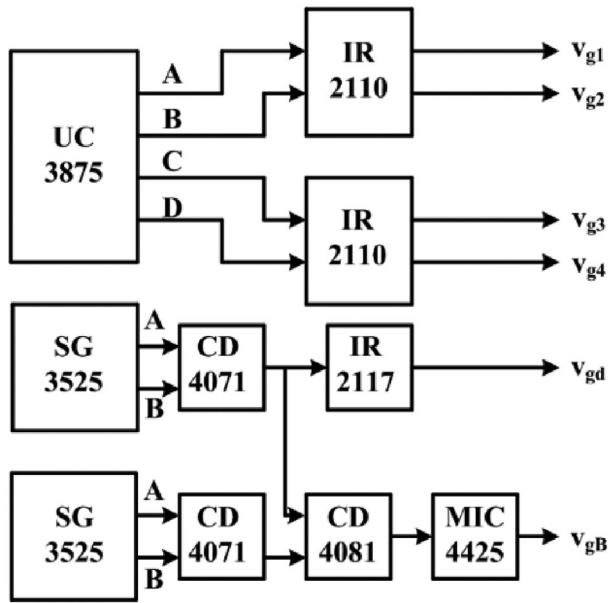


FIGURE 4 Block schematic of the control circuit for the proposed setup.

switches operate with ZVS, leading to less switching losses. Moreover, the current conducted by switches Q_1 and Q_2 represents the differential currents traversing L_1 and L_2 , resulting in diminished conduction losses in the switches due to the reduced

current magnitude. The suggested converter demonstrates great efficiency, achieving 96.26% under rated conditions due to its advantages.

A dimming control has been developed to evaluate the performance of the proposed converter under varying illumination levels. The computational and experimental outcomes of the proposed converter at 80% and 40% are presented below. Figure 9 illustrates the lamp current waveforms during simulation at 80% dimming, whereas the equivalent experimental lamp current waveforms are depicted in Figure 10. The current through each light is sustained at its operational value when the dimming switch is activated. Conversely, when the dimming switch is OFF, the current waveform decreases to zero. Experimental waveforms exhibit strong concordance with simulated waveforms, and efficiency is measured at 95.73% under 80% dimming conditions.

Figures 10 and 11 display both simulated and experimental current waveforms at 40% dimming. Experimental waveforms exhibit strong concordance with simulated waveforms, and efficiency is measured at 95.43% under 40% dimming conditions.

The suggested LED driver regulates lamp currents in response to variations in V_{DC} , V_{T1} , and V_{T2} by adjusting the duty cycle of the buck–boost converter at the input stage. Figure 12a illustrates the gate voltage of Q_{BB} , the inductor current i_{LBB} , and the capacitor voltage V_C when V_{DC} equals 12 V,

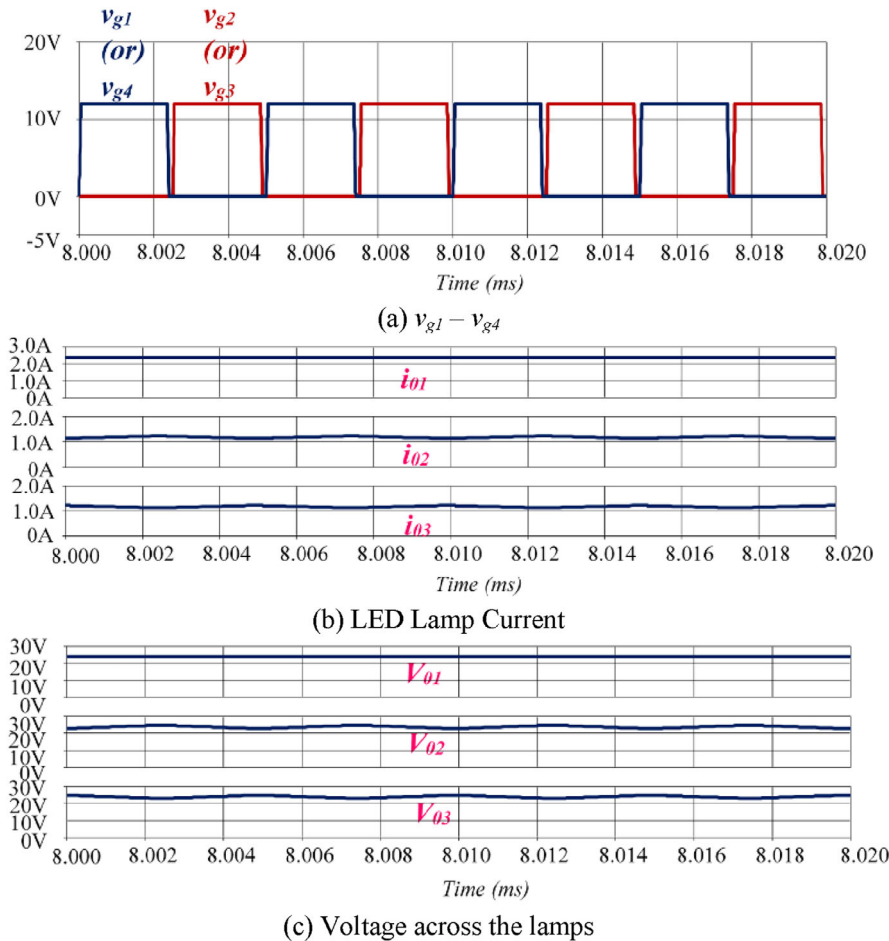


FIGURE 5 Gate voltages, current in light emitting diode lamps, and the voltage across the lamps at full illumination.

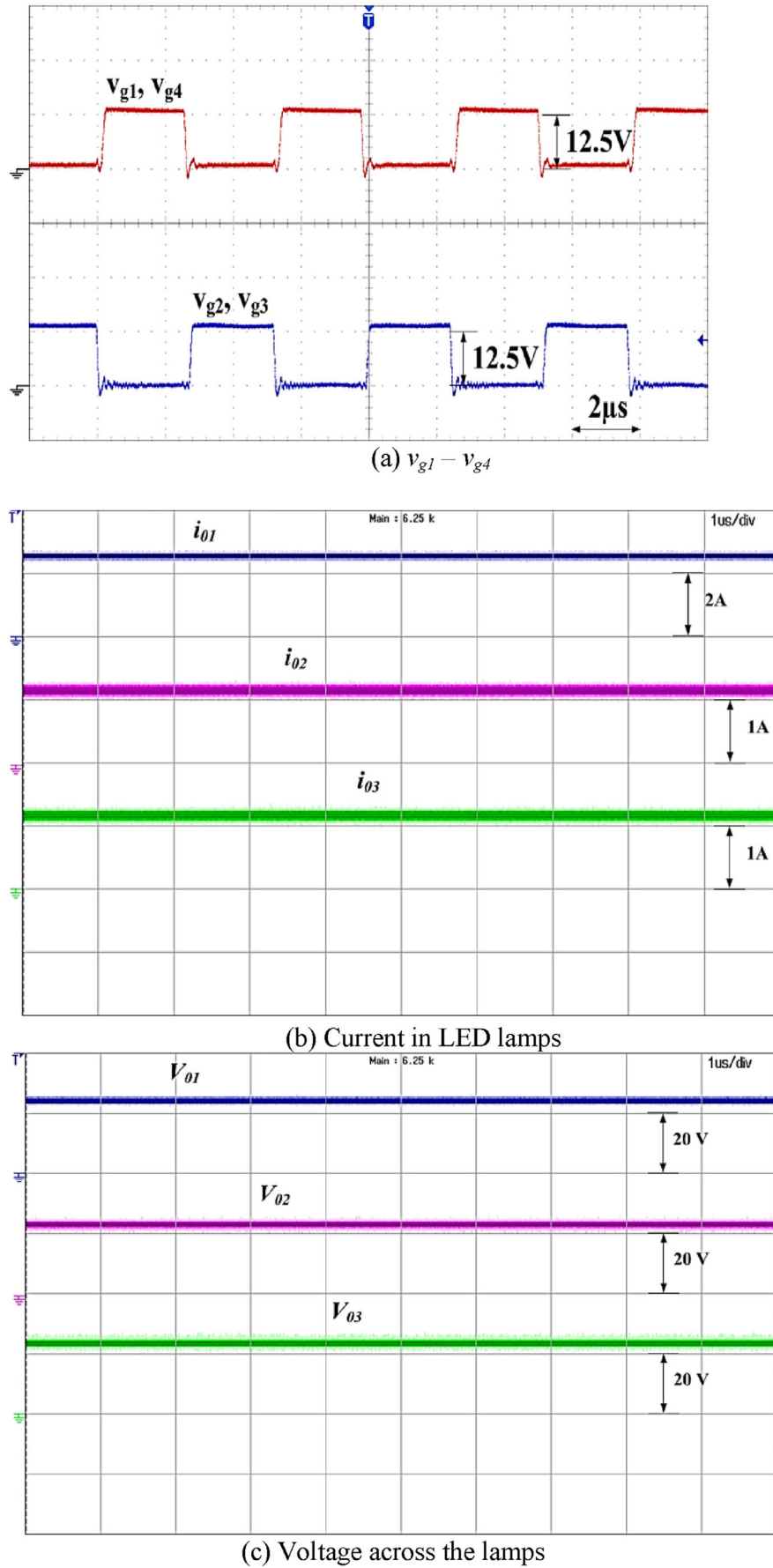


FIGURE 6 Gate voltages, current in light emitting diode lamps, and the voltage across the lamps at full illumination.

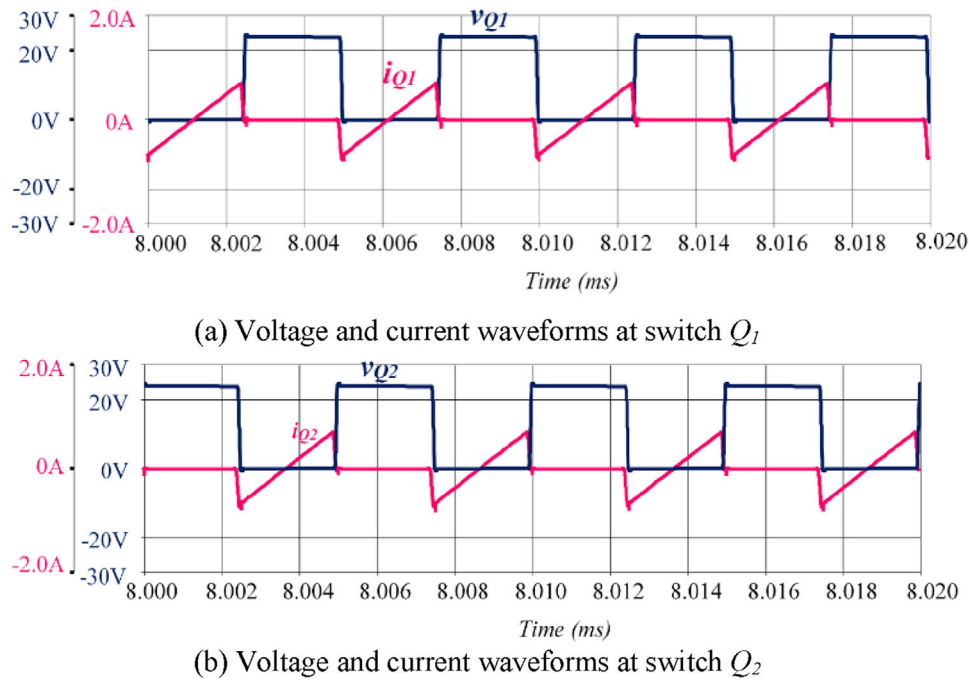


FIGURE 7 Switching waveforms in simulation at full illumination.

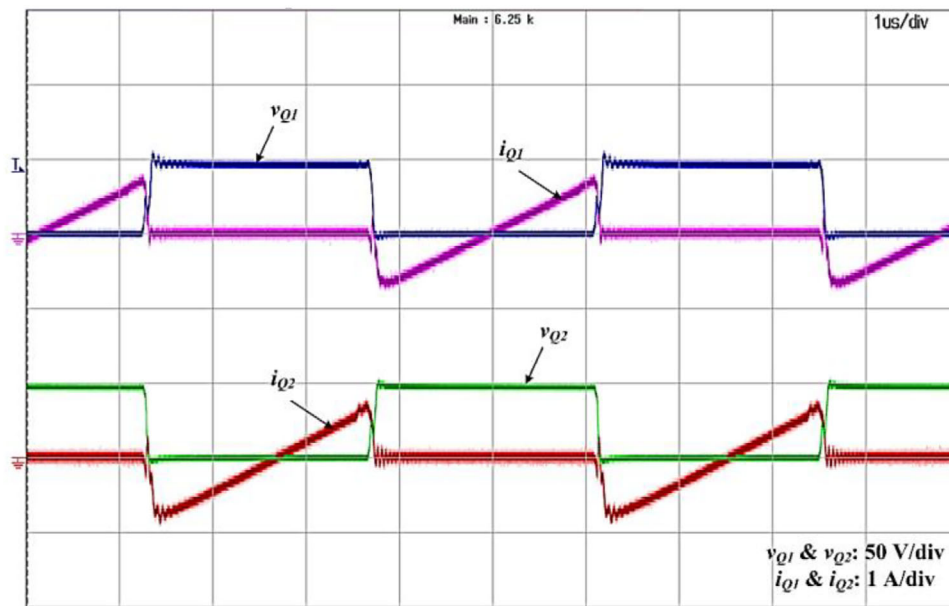


FIGURE 8 Switching waveforms at full illumination.

V_{T1} equals 12 V, and V_{T2} equals 12 V. The input voltage (V_{in}) to the bridge circuit is 23.82 V. If V_{DC} , V_{T1} , and V_{T2} voltages are augmented by 10%. Specifically, $V_{DC} = 13.2$ V, $V_{T1} = 13.2$ V, and $V_{T2} = 13.2$ V; hence, the duty cycle of the buck–boost converter is diminished to offset the voltage rise. The corresponding efficiency is determined to be 95.56%, with η_{gBB} , i_{LBB} , and V_C illustrated in Figure 12b. Likewise, if the voltages are diminished by 10%, the duty cycle is modified to enable the

capacitor to offset the reduction in voltage. Corresponding efficiency is found to be 94.21%, and η_{gBB} , i_{LBB} and V_C are shown in Figure 12c.

Figure 13 illustrates the measured efficiency of the proposed LED driver at different dimming settings. High efficiency is ensured at all dimming levels.

From Figure 13, it has been noted that regardless of the dimming level, good efficiency is assured.

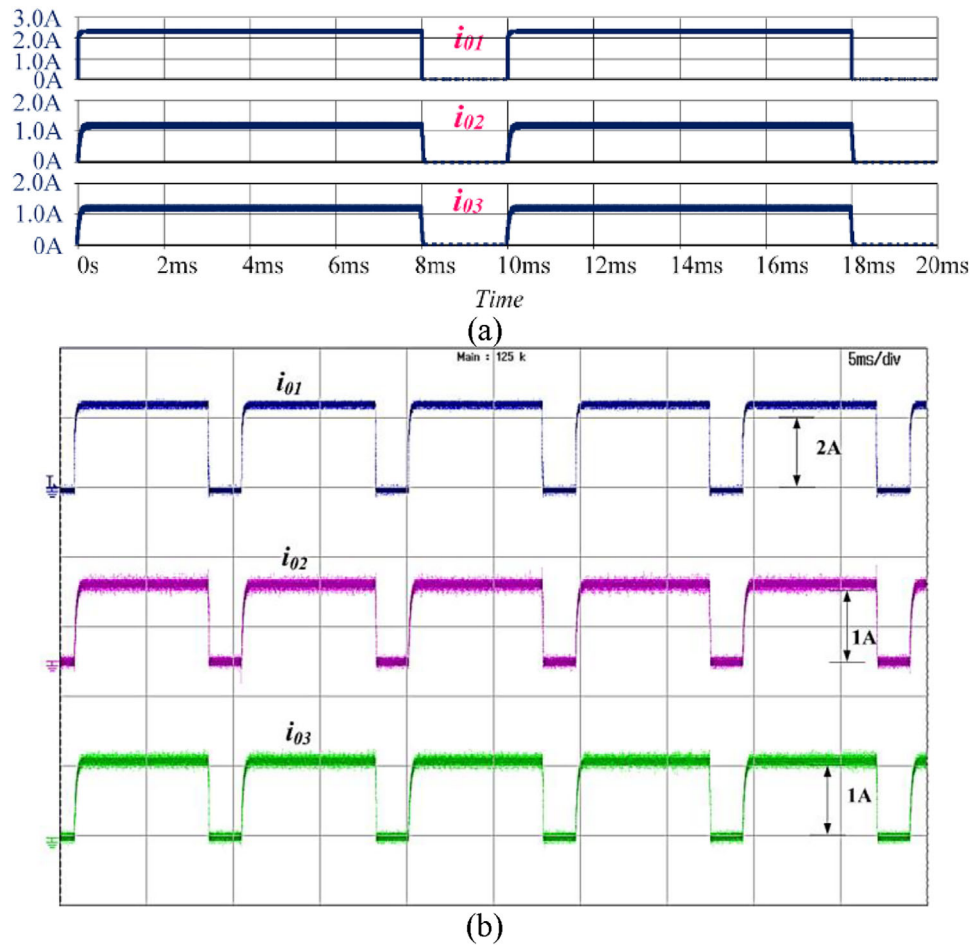


FIGURE 9 (a) Simulated current waveforms. (b) Currents through all the lamps at 80% dimming.

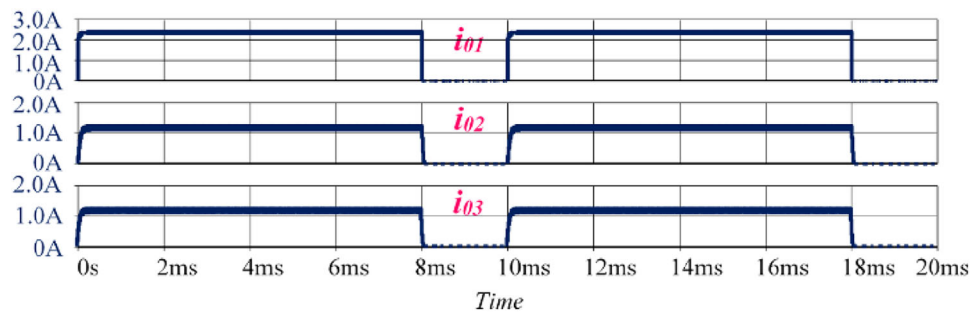


FIGURE 10 Simulated current waveforms.

A comparative analysis of the proposed topology and existing literature on LED lighting applications is presented in Table 2.

Following are the advantages of the proposed configuration compared to the other topologies:

- The suggested configuration omits the high-frequency transformer and rectifier step. It significantly diminishes the expense, mass, and dimensions.
- The number of power switches are comparable with other configuration.
- It involves soft switching also.
- High efficiency is assured at full illumination as well as during dimming conditions.
- In the proposed configuration, five inductors are present. However, two small inductors per one LED lamp are required to make LED current ripple free. This will not affect the size of the driver's circuit.
- Only one diode is used in the proposed configuration whereas other configurations use a greater number of diodes.
- There is only one capacitor of small value in the proposed configuration. Other configurations have more in number.

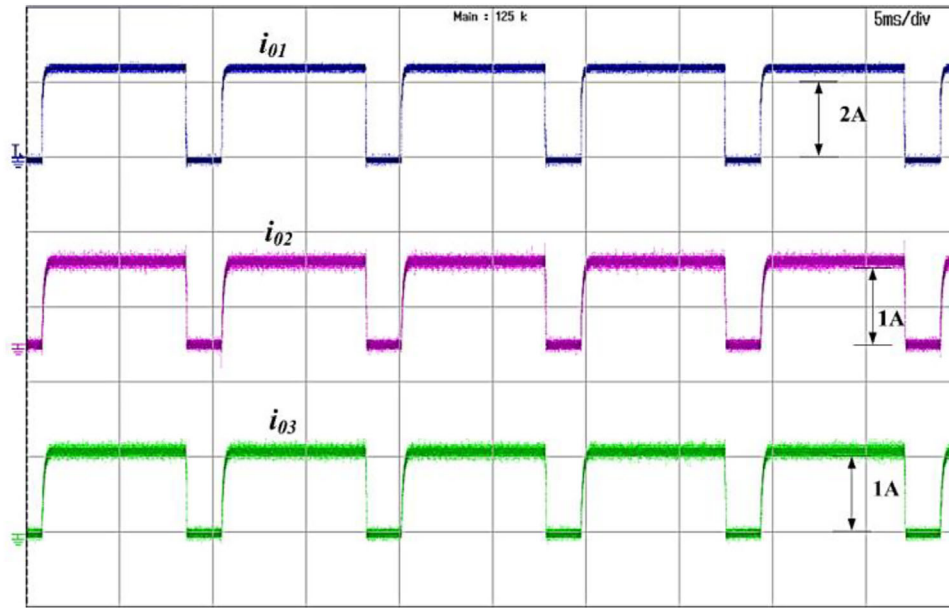


FIGURE 11 Currents through all the lamps at 80% dimming.

TABLE 2 Performance comparison of proposed topology with similar counterpart.

Parameter		[4]	[5]	[6]	[7]	[10]	[23]	Proposed
Number of components	S	3	4	6	2	4	4	6
	L	2	5	6	2	2	5	5
	D	8	2	1	4	4	2	1
	C	2	2	1	3	3	1	1
	T/F	0	1	0	0	0	1	0
Input voltage (V)		48	48	48	48	18–120	48	12
Output power (W)		50	142	145	23	23	145	112
Number of LED loads		2	4	4	1	1	4	3
Components count per lamp		7.5	3.5	3.5	11	13	3.25	4.33
Peak efficiency (%)		93.2	95.6	94.96	92.3	94.19	95.75	96.26
Device stress		$\frac{V_{DC}}{2}$	$>V_{in}$	$2V_{DC}$	$2V_{DC}$	$2V_{DC}$	$2V_{DC}$	$2V_{DC}$
Soft switching		Partial	Full	Full	Full	Full	Partial	Full

Abbreviations: C, capacitor; D, diode; L, inductor; S, switch; T/F, transformer.

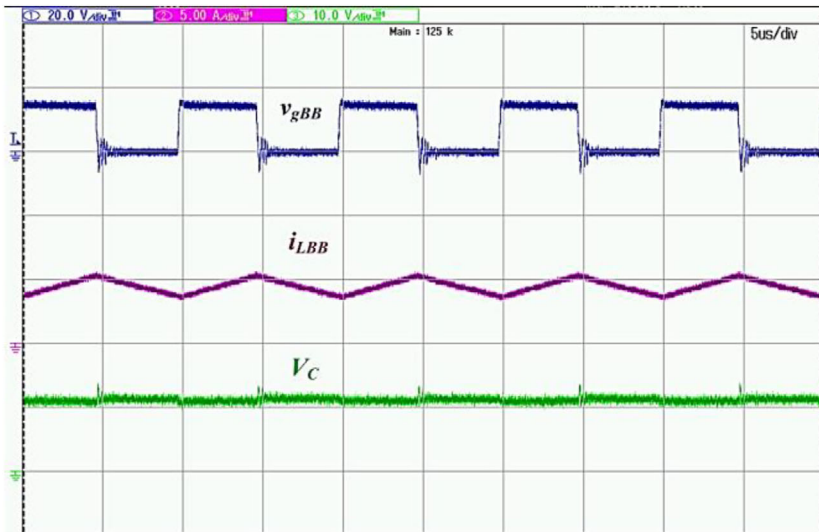
- The required input voltage is very less in the proposed configuration than other configurations.
- The voltage stress on switching devices will remain unchanged when the suggested arrangement is expanded to include additional LED bulbs.

7 | CONCLUSION

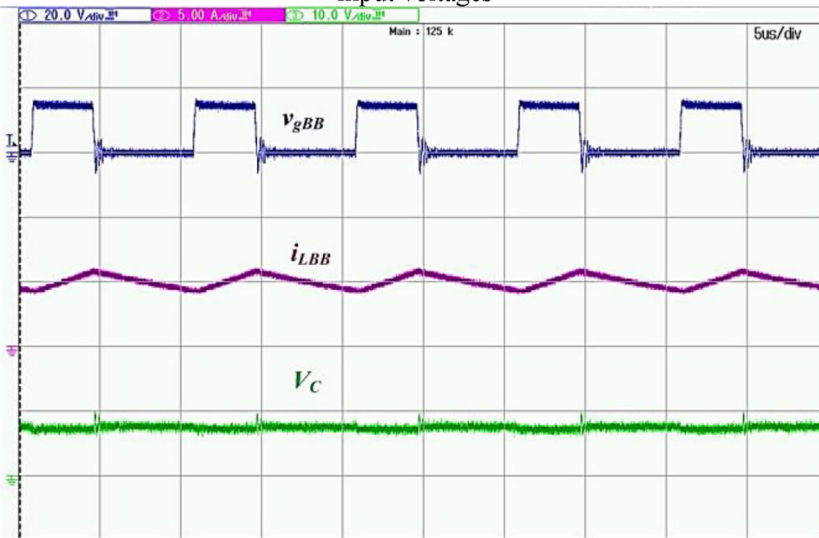
This article presents a ZVS full-bridge converter with a lower switch current for LED lighting applications. Comparing converter topologies suitable for LED applications shows the benefits of the proposed work. Experiments show that ZVS

LED driver switches conduct a little current, reducing conduction losses. All switching devices operate in ZVS, reducing switching losses. These qualities increase energy efficiency and reduce switching and conduction losses. This arrangement also reduces bulb component count and permits on–off dimming.

This work proposes a full-bridge converter designed to minimise device current stress while concurrently powering many LED bulbs. Detailed presentations of steady-state operating modes, analysis, design procedures, simulations, and experimental findings are provided. The proposed arrangement has an efficiency of 96.26% at rated power. The efficacy of the suggested LED driver is experimentally tested using a 112 W prototype. Additionally, a suitable comparison of analogous



(a) Gate voltage of Q_{BB} , inductor current i_{LBB} and capacitor voltage V_C at rated input voltages



(b) Gate voltage of Q_{BB} , inductor current i_{LBB} and capacitor voltage V_C at 10% increase in input voltages



(c) Gate voltage of Q_{BB} , inductor current i_{LBB} and capacitor voltage V_C at 10% decrease in input voltages

FIGURE 12 Experimental input voltage regulation waveforms.

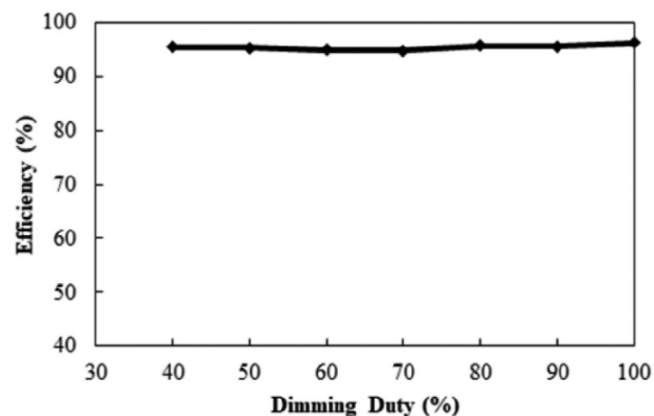


FIGURE 13 Measured efficiency curve of the proposed light emitting diode driver at various dimming levels.

converter topologies for LED applications is provided to substantiate the advantages of the suggested work. The primary benefits of the suggested arrangement include: (1) Decreased current stress on full-bridge devices, (2) Lower conversion power, (3) ZVS, (4) Enhanced conversion efficiency, (5) Input regulation for consistent light output, and (6) Capability to supply many LED bulbs. In this design, the current through the complete bridge switches is unaffected by the magnitudes of the lamp current. A modified standard buck–boost converter is employed to stabilise the input voltage for the management of lamp current. This topology may be appropriate for forthcoming direct current grid lighting applications. The proposed LED drivers can function using battery-operated and/or photovoltaic systems.

The future research scope includes the closed-loop control of the proposed four converter designs and the development of various control mechanisms for these setups. The research on novel converter topologies for upcoming energy processing systems and examination of suggested converter configurations for solar photovoltaic (PV) systems utilising the various MPPT algorithms can be made.

AUTHOR CONTRIBUTIONS

All authors contributed to the study conception and design. Material preparation, data collection, and analysis were performed by Kambhampati Venkata Govardhan Rao, Malligunta Kiran Kumar, B. Srikanth Goud, Ramanjaneya Reddy Udumula, Ch. Rami Reddy, Praveen Kumar Balachandran, Muhammad Ammirul Atiqi Mohd Zainuri, and Suganthi Ramasamy. The first draft of the manuscript was written by Kambhampati Venkata Govardhan Rao and all authors commented on previous versions of the manuscript. All authors read and approved the final manuscript.

ACKNOWLEDGEMENTS

Open access publishing facilitated by Università degli Studi di Cagliari, as part of the Wiley - CRUI-CARE agreement.

CONFLICT OF INTEREST STATEMENT

The authors declare no conflicts of interest.

DATA AVAILABILITY STATEMENT

The data that support the findings of this study are available from the corresponding author upon reasonable request.

ORCID

Kambhampati Venkata Govardhan Rao  <https://orcid.org/0000-0003-3808-0512>


Malligunta Kiran Kumar  <https://orcid.org/0000-0002-1154-9723>

B. Srikanth Goud  <https://orcid.org/0000-0002-5107-9738>

Ramanjaneya Reddy Udumula  <https://orcid.org/0000-0002-9176-2558>

Ch. Rami Reddy  <https://orcid.org/0000-0003-1941-0766>

Praveen Kumar Balachandran  <https://orcid.org/0000-0003-1561-1376>

Muhammad Ammirul Atiqi Mohd Zainuri  <https://orcid.org/0000-0001-9134-4869>

REFERENCES

- Li, S., Tan, S.-C., Lee, C.K., Waffenschmidt, E., Hui, S.Y., Tse, C.K.: A survey, classification, and critical review of light-emitting diode drivers. *IEEE Trans. Power Electron.* 31(2), 1503–1516 (2016)
- Pal, A., Saha, S.S.: Novel zero-voltage zero-current transition buck converter with minimal impact of active auxiliary cell on overall dynamics. *IEEE Access* 11, 3008–3023 (2023). <https://doi.org/10.1109/ACCESS.2023.3234590>
- Danyali, S., Shirkhani, M., Tavooosi, J., Razi, A.G., Salah, M.M., Shaker, A.: Developing an integrated soft-switching bidirectional DC/DC converter for solar-powered LED street lighting. *Sustainability* 15(20), 15022 (2023). <https://doi.org/10.3390/su152015022>
- Kolla, H.R., Vishwanathan, N., Murthy, B.K.: Independently controllable dual-output half-bridge series resonant converter for LED driver application. *IEEE J. Em. Sel. Top. Power Electron.* 10(2), 2178–2189 (2022)
- Kolla, H.R., Vishwanathan, N., Murthy, B.K.: Input voltage controlled full-bridge series resonant converter for led driver application. *IET Power Electron.* 13(19), 4532–4541 (2020). <https://doi.org/10.1049/ietpel.2020.0554>
- Kasi Ramakrishnareddy, C., Porpandiselvi, S., Vishwanathan, N.: Soft switched full-bridge light emitting diode driver configuration for street lighting application. *IET Power Electron.* 11(1), 149–159 (2018). <https://doi.org/10.1049/ietpel.2017.0021>
- Veeramallu, V.K.S., Porpandiselvi, S., Narasimharaju, B.L.: A buck-boost integrated high gain non-isolated half-bridge series resonant converter for solar pv/battery fed multiple load LED lighting applications. *Int. J. Circuit Theory Appl.* 48, 266–285 (2019). <https://doi.org/10.1002/cta.2720>
- Arias, M., Castro, I., Lamar, D.G., Vázquez, A., Sebastián, J.: Optimized design of a high input-voltage-ripple-rejection converter for LED lighting. *IEEE Trans. Power Electron.* 33(6), 5192–5205 (2018). <https://doi.org/10.1109/TPEL.2017.2727343>
- Kim, J.-W., Choe, J.-M., Lai, J.-S.J.: Non-isolated single-switch two-channel LED driver with simple lossless snubber and low-voltage stress. *IEEE Trans. Power Electron.* 33(5), 4306–4316 (2017)
- Veeramallu, V.K.S., Porpandiselvi, S., Narasimharaju, B.L.: A nonisolated wide input series resonant converter for automotive LED lighting system. *IEEE Trans. Power Electron.* 36(5), 5686–5699 (2021). <https://doi.org/10.1109/TPEL.2020.3032159>
- Wu, H., Wong, S.-C., Tse, C.K., Chen, Q.: A PFC single-coupled-inductor multiple-output LED driver without electrolytic capacitor. *IEEE Trans. Power Electron.* 34(2), 1709–1725 (2019)
- Elizondo, D., Barrios, E.L., Larequi, I., Ursúa, A., Sanchis, P.: Zero-loss switching in LLC resonant converters under discontinuous conduction mode: Analysis and design methodology. *IEEE Trans. Ind. Appl.* 59(3), 3576–3592 (2023). <https://doi.org/10.1109/TIA.2023.3250205>

13. Liu, X.L., He, M., Zhou, S., Meng, X., Zhou, Q.: Flicker-free resonant LED driver with high power factor and passive current balancing. *IEEE Access* 9, 6008–6017 (2021)
14. Salazar-Pérez, D., Ponce-Silva, M., Alonso, J.M., Aquí-Tapia, J.A., Cortés-García, C.: A novel high-power-factor electrolytic-capacitorless LED driver based on ripple port. *IEEE J. Emerg. Sel. Top. Power Electron.* 9(5), 6248–6258 (2021)
15. Pervaiz, S., Kumar, A., Afridi, K.K.: GaN-based high-power-density electrolytic-free universal input LED driver. In: *IEEE Energy Conversion Congress and Exposition (ECCE)*, pp. 3676–3683 (2017)
16. Rao, K.V.G., Kumar, M.K., Srikanth Goud, B.: An independently controlled two output half bridge resonant LED driver. *Electr. Power Components Syst.* 52, 1–21 (2023). <https://doi.org/10.1080/15325008.2023.2238695>
17. Tang, Y., Wu, Y., Chen, Z., Zhang, C., Hu, W., (2019), Hybrid mode control for wide range soft-switched full-bridge converter with auxiliary parallel inductor networks. *IET Power Electron.* 12, 1670–1678
18. Hsieh, Y.-C., Cheng, H.-L., Chang, E.-C., Huang, W.-D.: A soft-switching interleaved buck–boost LED driver with coupled inductor. *IEEE Trans. Power Electron.* 37(1), 577–587 (2022). <https://doi.org/10.1109/TPEL.2021.3093629>
19. Yasmin Taj, S., Yamuna, M., Revathi, V., Habeebullah Sait, H.: Comparative studies on switched capacitor based single phase multilevel inverter fed from PV systems for isolated applications. *Indian J. Eng.* 16, 300–312 (2019)
20. Hamidah, I., Ramadhan, D.F., Ramdhani, R., Mulyanti, B., Pawinanto, R.E., Hasanah, L., Nandiyanto, A.B.D., Yunas, J., Rusydi, A.: Overcoming voltage fluctuation in electric vehicles by considering Al electrolytic capacitor-based voltage stabilizer. *Energy Rep.* 10, 558–564 (2023)
21. Molavi, N., Farzanehfard, H.: A nonisolated wide-range resonant converter for LED driver applications. *IEEE Trans. Ind. Electron.* 70(9), 8939–8946 (2023). <https://doi.org/10.1109/TIE.2022.3210546>
22. Okara, I.C., Ahikwo, C.O., Anaya-Lara, O.: Modelling and analysis of modular multilevel voltage source converter using harmonic domain algebra. *J. Eng.* 18(50), 304–317 (2021)
23. Chandrasekhar, V., Vishwanathan, N.: Soft switched full-bridge DC-DC LED driver for street lighting. *Optik* 273, 170430 (2023)
24. Molavi, N., Askari, S., Farzanehfard, H., Khajehoddin, S.A.: Continuous input current isolated resonant LED driver with wide input voltage range. *IEEE Trans. Ind. Electron.* 71(9), 10486–10494 (2024). <https://doi.org/10.1109/TIE.2023.3337542>
25. Dasohari, M., Vishwanathan, N., Porpandiselvi, S., Vani, A.R.M.: A soft-switched boost converter based LED driver with reduced input current ripple. *IEEE Access* 12, 45904–45922 (2024). <https://doi.org/10.1109/ACCESS.2024.3377122>
26. Udumula, R.R., Vijayan, M., Reddy, C.K.R., Syed, M., Patakamoori, A., Gopichand, B.: A three leg asymmetrical voltage resonant converter with independent dimming control for multiple load LED lighting applications. *IEEE Trans. Ind. Appl.* 60(3), 4145–4155 (2024). <https://doi.org/10.1109/TIA.2024.3363676>
27. Molavi, N., Farzanehfard, H.: Load-independent hybrid resonant converter for automotive LED driver applications. *IEEE Trans. Power Electron.* 37(7), 8199–8206 (2022)

How to cite this article: Rao, K.V.G., Kumar, M.K., Goud, B.S., Udumula, R.R., Reddy, C.R., Balachandran, P.K., Zainuri, M.A.A.M., Ramasamy, S.: Zero voltage switching with reduced current stress for LED lighting applications. *IET Power Electron.* 18, e12832 (2025). <https://doi.org/10.1049/pe12.12832>